JOURNAL OF MECHANICAL ENGINEERING AND SCIENCES (JMES)
ISSN: 2289-4659 e-ISSN: 2231-8380
VOL. 15, ISSUE 1, 7907 – 7917
DOI: https://doi.org/10.15282/jmes.15.1.2021.24.0624

ORIGINAL ARTICLE

Acoustic scattering reduction in elastic materials with Bat optimization algorithm

Z.K.A. Algburi[1], C. Karatas[1]

[1] Mechanical Engineering Department, University of Turkish Aeronautical Association, Street No:11 06790 Etimesgut / Ankara, Turkey
Phone: +90312 5895500; Fax: 90 (312) 342 8460

ABSTRACT – A scattering-cancelation method is followed in this analysis. The opportunity to reduce the scattering effect in rigid cylinder with elastic cloaking material is investigated in the paper. The rigid cylinder with elastic cloaking and without elastic cloaking is analyzed for regular planes waves to test the scattering effect of the rigid cylinder. The energy due to reflected and travelled waves is presented mathematically. The parameter of the elastic cloaking such as thickness, density and Poisson ratio are optimized using BAT algorithm. Pressure filed of the rigid cylinder and directivity patterns scatter pressures in the cylinder are analyzed. The results revealed that, bat algorithm optimization provide the better results for elastic cloaking in the cylinder to reduce scattering effect.

ARTICLE HISTORY
Received: 18th Apr 2020
Revised: 24th July 2020
Accepted: 12th Aug 2020

KEYWORDS
Acoustic scattering; elastic material; Bat algorithm; optimization

INTRODUCTION

Reducing acoustic scattering is important in modern society, as it has been proven to be detrimental to human and animal health. A major source of noise pollution outdoors comes from motor vehicle exhaust systems. This motivates the study and design of systems that minimize structural vibration and passing acoustic noise through them. Some exhaust systems are fitted with a silencer, which is usually a section with perforations that allow the emissions to dissipate into the surrounding chamber prior to exiting. Unwanted indoor noise may occur in systems with heating, ventilation and air conditioning. Those are systems which use waveguides to carry air to heat, ventilate, or cool a room. The air is pushed by a fan that can produce unnecessary noise, and additional noise from outside will reach and spread within the waveguide. Such waveguides mostly have rectangular cross sections but circularity is not unusual for them. The study of vibration and acoustic propagation in circular cylindrical shells is therefore of continued importance for the engineering and applied mathematics fields. The effects of discontinuities especially on propagating waves.

Miles investigated the property of vibration acoustic wave in simple circular cylinder [1]. In this study, circular cylinder subjected in to plane wave and corresponding results were analyzed and also derive the acoustic propagation details in mathematically. Levine and Schwinger have developed the solution for reflection coefficient in cylinder duct [2]. The reflected energy of the acoustics wave analyzed in circular cylinder and the magnitude of the reflection is decreases in the radius of the cylinder.

Plane piston in the cylinder duct was tested and radiating sound energy was analyzed by Ingard [3]. The problem was addressed by observing the results at the open end of the behavior on the acoustic pressure field. The study covered the higher order modes. Karal found a zero order mode propagating in an infinite, static, cylindrical structure, and studied the equivalent impedance caused by a sudden shift in radius and a constriction between two ducts [4].

The sound propagation of two semi-infinite parts of a solid, cylindrical duct was analyzed at the sudden expansion field by Cummings [5]. The aim of this work was to determine which of two velocity profiles would be more appropriate to predict the coefficient of reflection. A system was studied for evaluating elements of rigid, cylindrical, exhaust silencers with mean flow by Munjal [6]. The goal was to create an expression for silencer attenuation. The analysis was formulated in terms of convective pressure and velocity of the convective mass.

Cargill found a cylindrical duct with a wall property that shifted from a static to a vortex layer and studied its effect on a propagating wave of planes [7]. This research used the technique of Wiener-Hopf to use higher order modes found and gave an explicit formula for the noise from the far field and the sound reflected. This was demonstrated how the presence of a mean flow allows the coefficient of reflection close to the center of the duct to decrease.

It was studied the effect of higher order modes provided by a rigid-walled expansion chamber by Ih and Lee [8]. This work established a theoretical solution for the problem by designing it as a lossless, rigid duct driven by pistons. Peat investigated the higher order modes produced at a discontinuity between two parts of stiff, cylindrical duct [9]. An analogous impedance circuit has been used to evaluate a mode of evanescence and to decide whether to use it. This work found the effects of superimposed mean flow up to the cut off and the effects of high frequencies. The results showed that mean flow effects were negligible but impedance variation with frequency was expected.

Lawrie and Abrahams [10] addressed sound wave radiation produced between two solid, coaxial, cylindrical ducts. The ducts were semi-infinite with the left duct having a radius less than the right one and an artificial distance between

*CORRESPONDING AUTHOR | Z. K. A. Algburi | ✉ engzeyad55@gmail.com

them was created. Forcing was by a wave incident against the distance, measuring the resulting reflected and transmitted wave fields.

F¨oller and Polifke proposed a procedure for determining the amplitudes of reflection and propagation of plane waves in discontinuous piping systems [11]. This approach considers a broad simulation of the eddy in a cylindrical duct with a single radius change. Externally the test immediately excites seismic waves at each end of the discontinuity. The associations between acoustic waves are described in depth, and the question is solved in determining the wave amplitudes scattered at discontinuity. The simulation findings are comparable to other observational approaches which indicate strong consent to the experimental evidence.

Lawrie [12] found an infinite transparent cylindrical structure where the structure had a finite number of ring restrictions and the device was completely filled by a compressible inviscid fluid. The versatile shell vibrations were modelled using the Donnell-Mushtari equations of motion as Junger and Feit reported in [13]. First, a single ring restriction was considered and the exact solution was sought by defining the problem of limit value and resolving the resulting linear structure. The problem was presented as a symmetric and antisymmetric problem for two ring constraints which led to the uncoupling of terms, the exact solution could then be sought by solving the two resulting linear systems.

Stepanishen and Tougas studied the time-dependent pressure for a fluid filled, finite, open ended, cylindrical shell [14]. To push the fluid in the machine a piston source situated at the shell's inner closed end was used. The piston was supposed to provide amplitude of the gated sine wave that matched a spatial pattern. The solution was sought by using a Green time-space function to construct a problem with limit value. Zhang and Abrahams [15] used a modified Wiener-Hopf technique to investigate the sound radiated from a finite fluid-charged cylindrical finite container. The shell was easily immersed in a compressible stagnant stream, and its motions were modelled for a thin, cylindrical shell using the Donnell-Mushtari motion equations. Fluid pressing was created by an axisymmetric ring stress, between the shell's open ends.

From the literature survey, there is ample scope for research in the scattering effect in the cylinder and also scope for optimization to reduce the reflection effect in the cylinder with cloak. In this paper, bat algorithm optimization used to reduce the scattering effect in the cylinder. The organization of paper as follows; methodology used for this paper is explained in the section 2. Experimental verification of the proposed system is described in the section 3. Concluding remarks is given in the section 4.

METHODOLOGY

In this section energy transmitted and reflected in the cylinder is derived in the form of mathematical equation. The concerns in this chapter consider a circular, cylinder defined in cylindrical polar coordinates [16]. The duct wall has the rigid structure, resulting in an axisymmetrical framework. The θ coordinate is then dropped. The interior field includes a compressible sound level fluid c and density ρ. A harmonic time factor, $e^{-i\omega t}$ range, is assumed whenever t is time and range = ck, where k is the wave number of fluid. The Helmholtz equation shall give the governing equation for the interior area,

$$\left\{\frac{\Delta^2}{\Delta \bar{r}^2}+\frac{1}{r}\frac{\Delta}{\Delta \bar{r}}+\frac{\Delta^2}{\Delta \bar{z}^2}+k^2\right\}\bar{\phi}=0 \tag{1}$$

where the dimensional velocity potential of the fluid is $\bar{\phi}$. This potential for velocity is a scalar function which had a gradient equal to the fluid velocity [17]. This can be used to describe the future potential, such as:

$$\bar{p}=i\omega\rho\bar{\phi} \tag{2}$$

Where the aspect pressure is $\bar{p}$. As standard time and length scales, it is useful to non-dimensionalize the dimensional variables with respect to both ω^{-1} and k^{-1}. In terms of their non-dimensional counterparts, the dimensional variables are then,

$$k\bar{r}=r, k\bar{z}=z, k^2\bar{\phi}=\omega\phi \tag{3}$$

Consequently the non-dimensionalized governing equation is:

$$\left\{\frac{\Delta^2}{\Delta r^2}+\frac{1}{r}\frac{\Delta}{\Delta r}+\frac{\Delta^2}{\Delta z^2}+1\right\}\bar{\phi}=0 \tag{4}$$

where, ϕ is the potential of non-dimensional fluid velocity. The method of separating variables is used to evaluate the velocity potential, which depends on r and z and thus takes the form:

$$\phi=R(r)Z(z) \tag{5}$$

The ϕ is substitute in the Eq. (4), finally we get,

$$\frac{1}{R}\frac{\Delta^2 R}{\Delta r^2}+\frac{1}{rR}\frac{\Delta R}{\Delta r}+1=-\frac{1}{Z}\frac{\Delta^2 Z}{\Delta z^2} \tag{6}$$

The right side of the Eq. (6) is considers as negative separation constant and it will oscillates in the z direction and it consider as,

$$-\frac{1}{Z}\frac{\Delta^2 Z}{\Delta z^2}= S^2 \tag{7}$$

The '*S*' is the separation constant and expressed by the Euler's formula as,

$$Z(z)=Ce^{isz}+De^{-isz} \tag{8}$$

where, *C* and *D* are consider as arbitrary constant. When considering, C=1 and D=0 then the wave propagating only in positive direction and equation become [18],

$$Z(z)=Ce^{isz} \tag{9}$$

The Z(z) is substitute in the Eq. (6) and equation become,

$$r^2\frac{\Delta^2 R}{\Delta r^2}+r\frac{\Delta R}{\Delta r}+r^2(1-S^2)R=0 \tag{10}$$

The expression above is known as the differential equation of Bessel and the velocity potential can be expressed by,

$$\phi_n=\sum_0^\infty A_n J_0(k_n r)e^{is_n z} \tag{11}$$

where, A_n and S_n are the amplitude of the nth wave and wavenumber.

A terminology for the energy propagating through a cylinder is necessary to determine whether the energy is reflected and/or travelled at a discontinuity [19]. Because cylinder cannot hold energy, it only considers the energy in the fluid. The dimensional power is generated by the integration of the pressure compounded by the dynamic conjugation of the velocity over the cross section is given by,

$$\varepsilon=real\left[\int_0^a i\phi\left(\frac{\Delta\phi}{\Delta z}\right)^* r\Delta r\right] \tag{12}$$

On substituting velocity potential Eq. (11) into Eq. (12) we get,

$$\varepsilon_n=real\left[\int_0^a iA_n J_0(k_n r)e^{is_n z}\{is_n A_n J_0(k_n r)e^{is_n z}\}^* r\Delta r\right] \tag{13}$$

It can be expressed as follows,

$$\varepsilon_n=real\left[s_n|A_n|^2\int_0^a J_0^2(k_n r)r\Delta r\right] \tag{14}$$

From the Eq. (14), we write wave scattering energy and travelled energy as follows,

$$\varepsilon_A=real\left[\sum_{m=0}^{M}|A_m|^2 s_m C_m\right] \tag{15}$$

$$\varepsilon_B=real\left[\sum_{m=0}^{M}|B_m|^2 \eta_m D_m\right] \tag{16}$$

where, A_m is amplitude of the scatter wave and B_m is the amplitude of the travelled wave, S_m and η_m are the wave number of the scatter and travelled wave. C_m and D_m are given by following equation,

$$C_m=\frac{a^2 J_0^2(k_m a)}{2} \tag{17}$$

$$D_m=\frac{b^2 J_0^2(\gamma_m b)}{2} \tag{18}$$

where, "*a*" is radius of the outer cylinder, "*b*" is the radius of the inner cylinder, k_m and γ_m are given by,

$$k_m = (1 - S_m^2)^{(1/2)} \tag{19}$$

$$\gamma_m = (1 - \eta_m^2)^{(1/2)} \tag{20}$$

While considering the thickness "h" of the cloaking material and the characteristic equation of the wave motion in the cylinder as follows,

$$\frac{v}{\bar{a}}\frac{\Delta\bar{u}}{\Delta\bar{z}} + \frac{1}{\bar{a}^2}\frac{\Delta\bar{v}}{\Delta\theta} + \frac{\bar{\omega}}{\bar{a}^2} + \frac{h^2}{12}\frac{\Delta^4\bar{\omega}}{\Delta\bar{z}^4} + \frac{2h^2}{12\bar{a}^2}\frac{\Delta^4\bar{\omega}}{\Delta\bar{z}^2\Delta\theta^2} + \frac{h^2}{12\bar{a}^4}\frac{\Delta^4\bar{\omega}}{\Delta\theta^4} - \frac{\omega^2\bar{\omega}}{c_s^2} - \frac{\bar{p}(\bar{a},\bar{z})}{c_s^2\rho_s h} = 0, \bar{r} = \bar{a} \tag{21}$$

Longitudinal, circumferential and radial cloaking material displacements are denoted by $\bar{u}, \bar{v}\ and\ \bar{w}$. Poisson ratio is denoted "υ", the sound speed of the cloaking material "c_s" is given by the following equation,

$$c_s = \sqrt{\frac{E}{(1-\upsilon^2)\rho_s}} \tag{22}$$

where, "*E*" is the young's modulus and ρs is the density of the cloaking material [20]. From the Eq. (21) is noted that, the reflected energy equation is depends three variable such as thickness of the cloaking material (h), Poisson ratio (υ) and density of the cloaking material (ρs). in this paper this will consider as optimize parameter to reduce the scatter effect in the cylinder and gain value of the Eq. (15) consider as the fitness function of the optimization problem and it is given as,

$$Fitness = 20 \times \log(\varepsilon_A)\ db \tag{23}$$

The thickness, density and Poisson ratio optimized using BAT algorithm. The basic of BAT algorithm is explained in the next section.

The bat algorithm takes advantage of bats 'echolocation activity. Such bats emit a very loud sound pulse (echolocation), and listen to the echo that echoes back from the objects around them. Their amplitude of the signals varies according to nature. Each sound signal has an emission rate of pitch, loudness, and duration. Some bats use tuning frequency signals while the majority use fixed frequency signals. Such animals have a frequency range of between 25 KHz and 150 KHz. Bat algorithms are based on the following aspects; both bats use echolocation and the distinction between victim and obstacle is separated. Bats travel at random speed, at a random venue, with variable length, loudness and pulse emission rate [21-22]. The traditional bat algorithm has many advantages and one of the main advantages is that, by moving from discovery to exploitation, it can provide very rapid convergence at a very initial stage. This makes it an effective algorithm for applications that need a simple solution, such as classifications and others. The flowchart for the BAT algorithm is shown in the Figure 1.

Step 1:

Initialize the BAT position Xi=X1, X2, X3…Xd, initialize the BAT velocity Vi=V1, V2, V3…Vd. Where, d is the number of optimizing parameter of the system. The next process to find out the objective function value (F(i)) for the initial BAT position (Xi) i.e.,

$$X(i) = rand(n,d); n\ is\ the\ number\ BAT\ population \tag{24}$$

$$V(i) = rand(n,d); n\ is\ the\ number\ BAT\ population \tag{25}$$

$$F(i) = f(X(i)) \tag{26}$$

After finding objective function value store the result and corresponding bat positions for further manipulation of the bat algorithm.

Step 2:

Define values for the pulse frequency of the BATs (Q_i), Pulse rate of the BATS (r_i) and loudness factor of the bats (A_i)

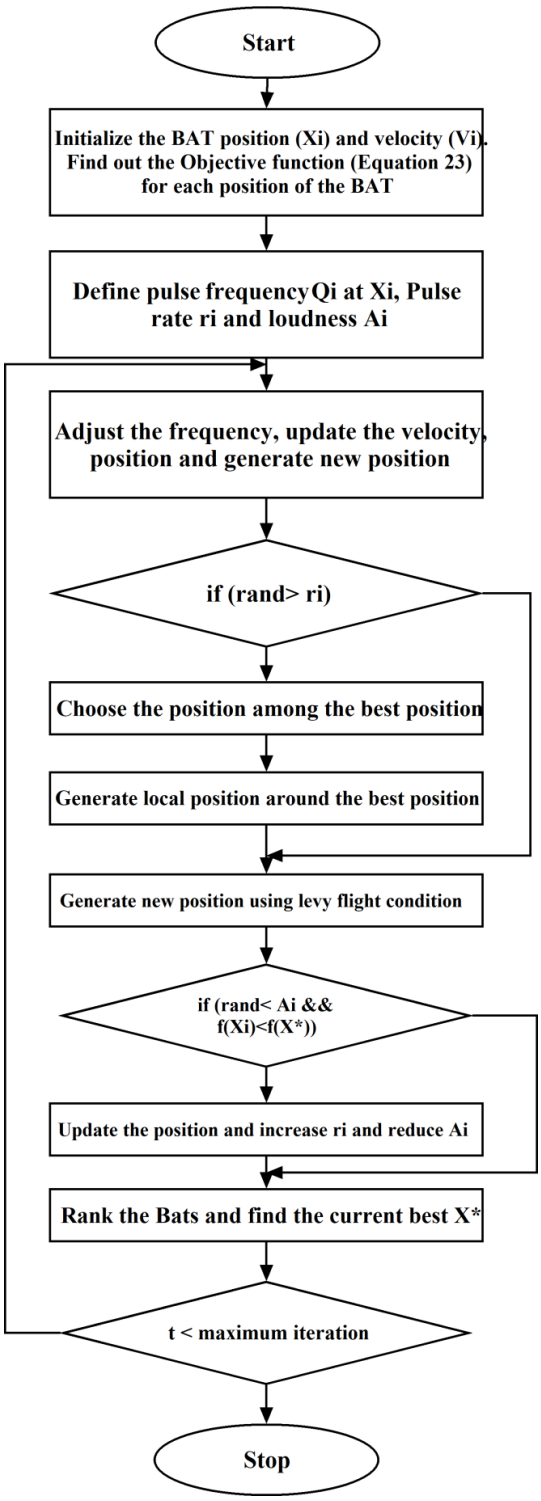

Figure 1. Flowchart for the Bat algorithm

Step 3:

Bat algorithm main loop is start at step 3. In this loop iteration count set as 1. Maximum iteration for the main loop fixed here.

Step 4:

Adjust the frequency parameter of the BATS using minimum and maximum frequency value and given by following equation,

$$Q_i = Q_{min} + (Q_{max} - Q_{min}) \times rand(n, d) \quad (27)$$

where, Q_{min} is the minimum frequency of the bat, Q_{max} is the maximum frequency of the bat and rand (n,d) is the rand number between zero to one.

Update the velocity of the bat using best position and frequency of the bat positions. It is given in the following equation

$$V(t) = V(t-1) + (X(t-1) - X^{*})Q_i \tag{28}$$

where, V(t) is the current iteration velocity, V(t-1) is the previous iteration velocity, X(t-1) is the previous iteration bat positions, X^{*} is the best position among all bat position and Q_i is the frequency of the bats.

Update the position of the bats using updated velocity of the bats and it is described by using following equation,

$$X(t) = X(t-1) + V(t) \tag{29}$$

The best position for the bat is derived from the old position added with loudness factor of the bats and it is expressed in the following equation,

$$X(new) = X(t) + rand \times A_i(t) \tag{30}$$

Step 5:

In the step, pulse rate of the bats are compared with random pulse rate. If the pulse rate less than random pulse rate then choose solution among the best solution of the problem and also create the local solution around the best solution selected. After that update the pulse rate and loudness factor of the bats using following equations,

$$r_i(t) = \delta \times r_i(t-1), \qquad A_i(t) = A_i^0\left(1 - e^{(-\emptyset t)}\right) \tag{31}$$

where δ and $\emptyset$ are random numbers.

For considering the values for δ and $\emptyset$ $0 < \delta < 1$ and $\emptyset > 0$, and consider iteration reach infinite then pulse rate and loudness factor becomes,

$$t \to \infty, r_i(\infty) \to 0, \qquad A_i(\infty) = A_i^0 \text{ as} \tag{32}$$

Create the new solution using levy flight conditions in this step.

Step 6:

If (rand < A_i & F (Xi) < F(X*))

In this step, compare the loudness factor with random loudness factor and also compare the current solution with best solution if both conditions are satisfied then increase the pulse rate of the bats and reduce the loudness factor of the bats as in the equation (30).

End if

Sort the bats solution and determine the current best solution X*.

End while

Loop end

Step7:

Display the best results from the bat algorithm.

RESULTS

In order to verify the scattering reduction behavior in the cylinder object, MATLAB software used for create the program to measure and analyze the reflected energy of the acoustics wave in the cylinder with cloaking and without cloaking conditions. MATLAB 2017b version used for simulation in the i3 Intel processor having 1.7GHz speed personal computer. For the elastic layers, optimization techniques were used to identify dimensional and mechanical characteristics that lead to a reduction in scattering. For cloaking layer, those parameters which constitute the variables of optimization are:

- The thickness (h) of the cloaking material
- Poisson's ratio (υ) of the cloaking material
- The mass density (ρ_s) of the cloaking material

The parameter used for the acoustics wave analysis in the cylinder is given in the Table 1.

Table 1. Parameter used for the acoustics wave analysis in the cylinder

S.NO	Description	Value	Unit
1	Dimensional radius of the cylinder (a)	0.2	Meter
2	Dimensional radius outer layer of the cylinder (b)	0.28	Meter
3	Sound speed of fluid	343.5	m/s
4	Density of fluid	1.2	(kg/m^3)
5	Young's Modulus	7.2×10^{10}	(N/m^2)
7	Dimensional cloaking material thickness	To be optimized	Meter
8	Density of cloaking material	To be optimized	(kg/m^3)
9	Poisson ratio of cloaking material	To be optimized	-

The response of the scattering gain of the without cloaking material with different frequency is shown in the Figure 2. From this analysis, it is shows that the scattering gain is high with different frequency of the acoustics wave and need cloaking action for reduce the scattering gain of the acoustic wave through the cylinder.

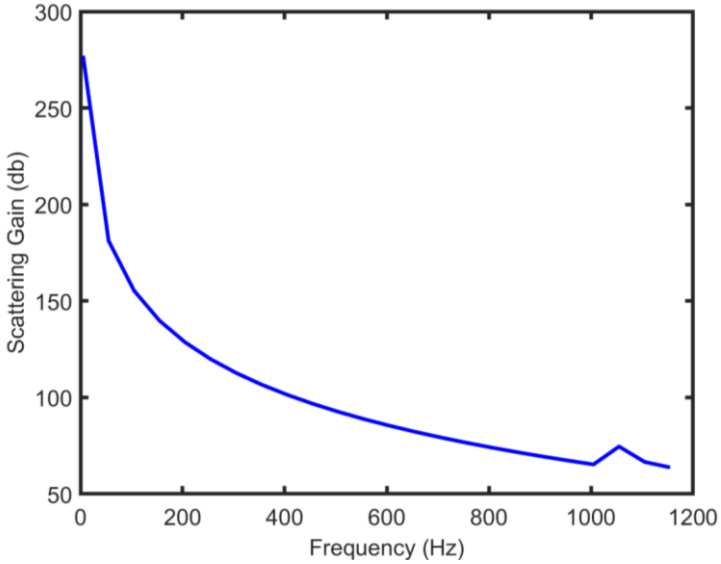

Figure 2. Scattering gain for the without cloaking material

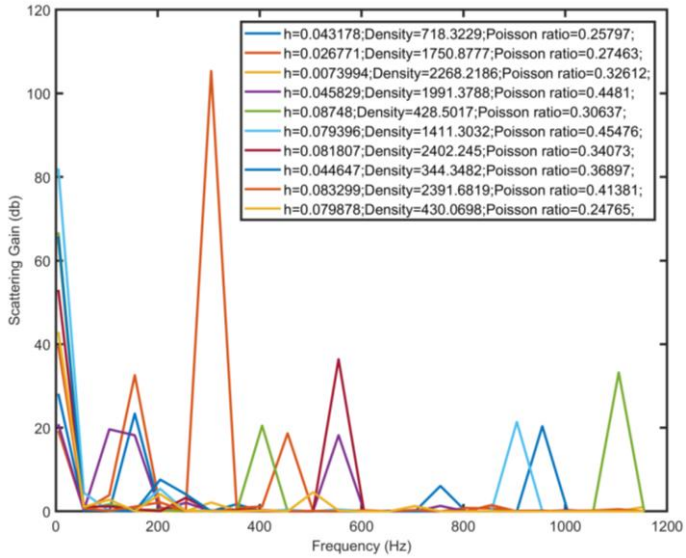

Figure 3. Scattering gain with random value of thickness, density and Poisson ration of the cloaking material

The initially, ten random number were assigned for cloaking material thickness, cloaking material density and cloaking material Poisson ratio and corresponding scattering gain value is measured with respect to acoustic wave frequency variation from 1 Hz to 1200 Hz. The result of this analysis is shown in Figure 3. From this analysis, it is shows that, scattering gain values are zero in some acoustic frequency and it has high value for some other frequency. So random optimization not possible to find out the optimal values for the given objective problem. For that purpose, bat algorithm used here to find out the optimal value for the cloaking material thickness, density and Poisson ratio. The parameter used for the BAT algorithm is shown in the Table 2.

Table 2. Parameter of the BAT Algorithm

S.NO	Description	Parameter of the Bat algorithm	
1	Generation	t	100
2	Population size	n	20
3	Number of parameter	d	3
4	Random number	δ and $\emptyset$	0.9
5	Pulse rate	r	0.5
6	Loudness Factor	A^0	0.5
7	Minimum Frequency	Q_{min}	0
8	Maximum Frequency	Q_{max}	2

The bat algorithm executed with t=100 generation, n=20 population and TR=1000 trial then bat algorithm finds the 2000000 solution ($S = t \times n \times TR = 2000000$) for 1000 trial. Each trial results are stored and analyzed in detailed.

Table 3. Result of the BAT algorithm optimization

Thickness	Density	Poisson ratio	Best Fitness	Worst Fitness	Mean	Standard Deviation	Computation time (minutes
0.0935	2827.1463	0.425	0.43273	0.542	0.4623	0.0615	32.2

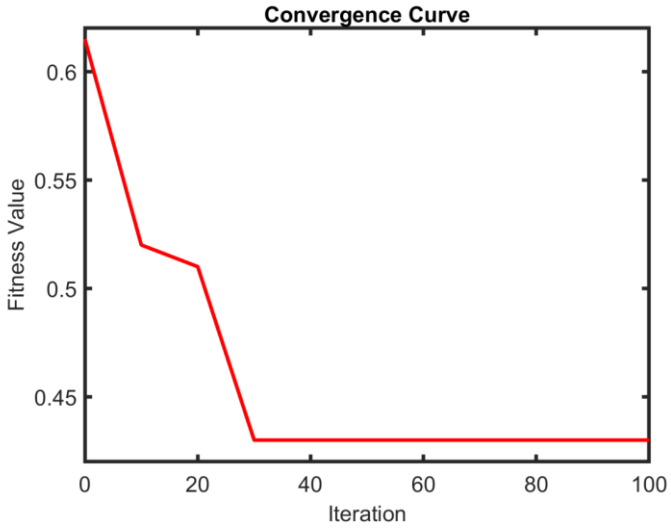

Figure 4. Convergence curve of the BAT algorithm

The results from the BAT algorithm are shown in the Table 3. The convergence graph for the BAT algorithm optimization is shown in the Figure 4. Table 3 shows the optimal value of thickness, density and Poisson ratio of the cloaking material. The time required for single trail is 30 minutes. Best fitness value, worst fitness value, mean value and standard deviation for the 1000 trails also presented in the Table 3. From the convergence graph, the fitness value is minimized every iteration and global value reached after 25 iteration.

The system is tested with optimized values and corresponding results are measured and analyzed. The variation of the scattering gain with respect to frequency for without cloaking and with cloaking is shown in the Figure 5. From this figure, It is shows that the scattering gain value is reduced when using cloaking material around the cylinder than the without cloaking around the cylinder.

Figure 6(a) shows the sound pressure field in the cloaked cylinder and without cloaked cylinder. The pressure around the shrouded cylinder ranges between 0.9 and 1.1 Pa with an incident plane wave with amplitude p0= one Pascal, particularly in the abrupt proximity of the cloaked cylinder anywhere it is concentrated around 1.1 Pa to 1.2 Pa. Association with the rigid cylinder condition, in which the pressure field took values around 0.4 and 1.8 Pa, indicates the tool output at this level. The cloaked cylinder's "averaged visibility", as described in [12] for characterizing the cloaking efficiency, is about 0.04 near the cylinder and 0.1 everywhere else.

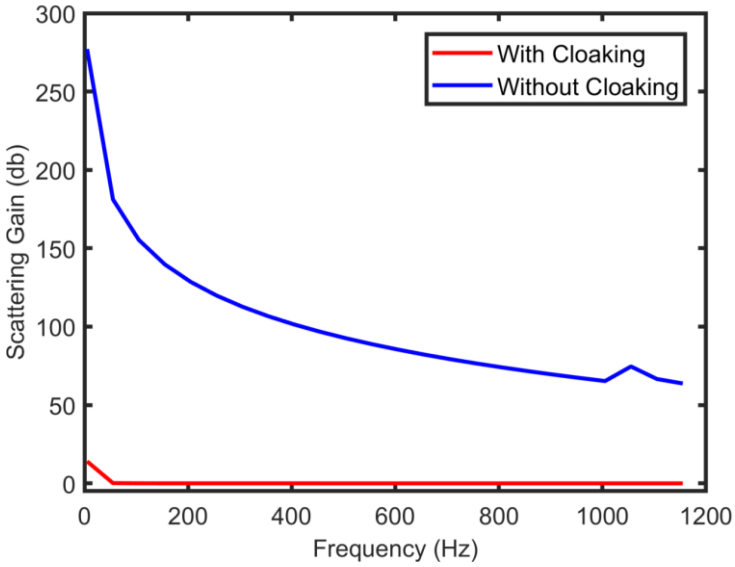

Figure 5. Graph between scattering gain (dB) verse frequency

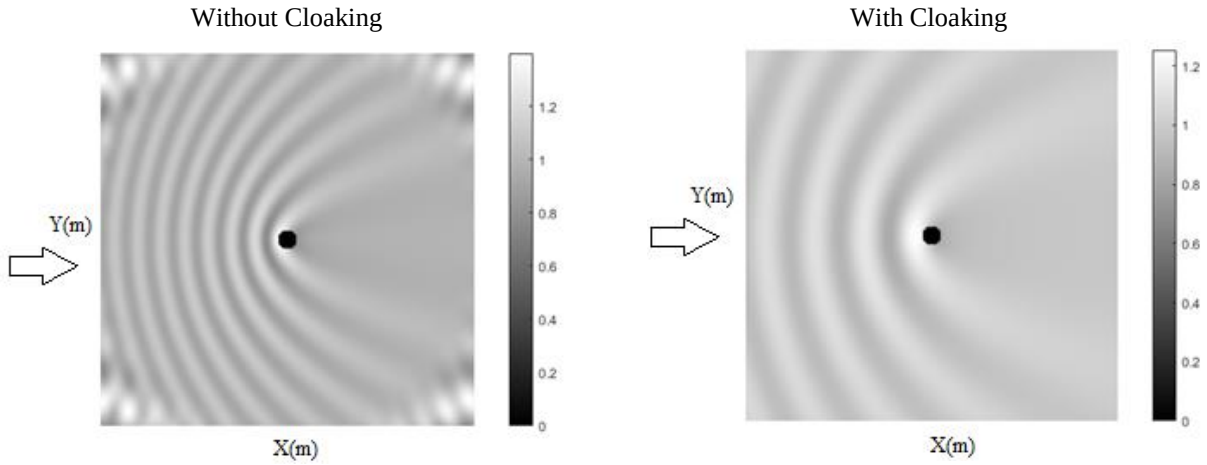

(a) Pressure field in the rigid cylinder.

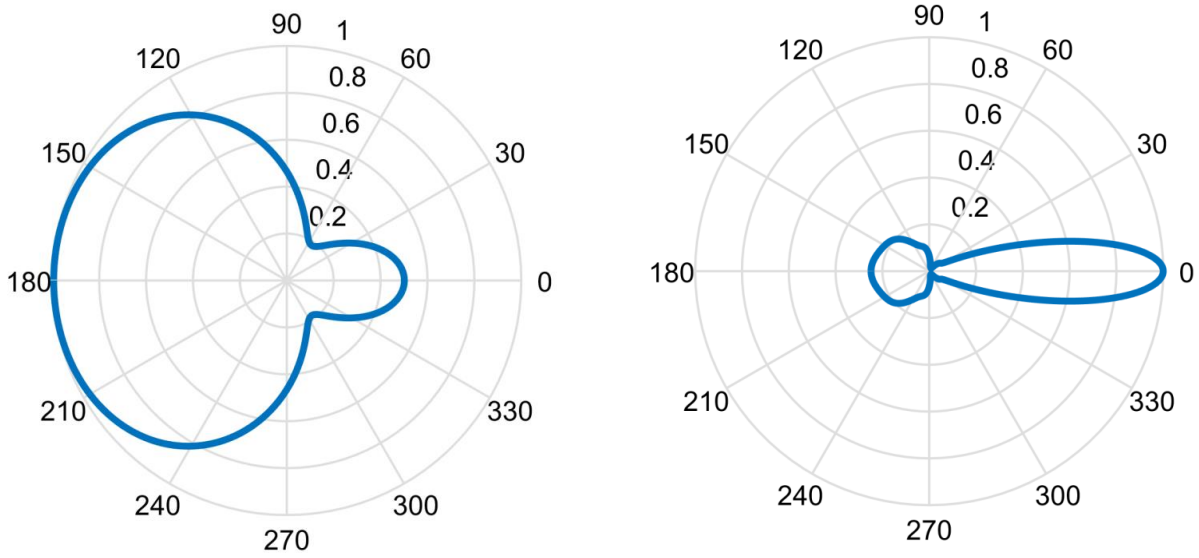

(b) Scattered pressure in directive patterns

Figure 6. (a) Pressure field in the rigid cylinder and (b) Scattered pressure in the directive patterns.

From the directivity patterns of scatter pressure analysis shown in Figure 6(b), it is observed that reduction in scattering pressure in the cloaked cylinder than without cloaked cylinder. Using this cloaking material reduces the distant field diffraction in the direction of 180°, i.e. to the side of the wave of the event. Diffraction at the back of the cylinder is also high, for angles around 45° and 75° and 305° and 335°. The reduction of scattering gain is important in the all directions: change in the amplitude of the diffracted pressure falls from the average value of one when considering without cloaking to the amplitude smaller than 0.1 with cloaking.

CONCLUSIONS

This paper presented the bat algorithm optimization of the acoustics wave scattering gain reduction in the rigid cylinder. The overall system was created using MATLAB Simulink software. Bat algorithm was used to optimize the parameter of the cloaking material such as thickness, density and Poisson ratio of the cloaking material. Detailed and rigorous analysis was presented in the paper. From the test results, the scattering gain is completed reduced in cloaked cylinder (around 1-5 db) than without cloaked cylinder (50-100 db). Bat algorithm effectively optimizes the problem with less iteration and BAT algorithm is suitable algorithm for this kind of problem.

ACKNOWLEDGMENTS

The authors would like to acknowledge the University of Technology in Baghdad, Ministry of Higher Education Iraq for research grants and funding.

REFERENCES

[1] J. W. Miles, "The analysis of plane discontinuities in cylindrical tubes. Part I", *J. Acoust. Soc. Am.*, vol. 17, no. 3, pp. 259–271, 1946, doi: 10.1121/1.1916327.

[2] H. Levine and J. Schwinger, "On the radiation of sound from an unflanged circular pipe", *Phys. Rev.*, vol. 73, no. 4, p. 383, 1948, doi: 10.1007/3-540-29224-1_26.

[3] U. Ingård, "On the radiation of sound into a circular tube, with an application to resonators", *J. Acoust. Soc. Am.*, vol. 20, no. 5, pp. 665–682, 1948, doi: 10.1121/1.1906424.

[4] F. C. Karal, "The analogous acoustical impedance for discontinuities and constrictions of circular cross section", *J. Acoust. Soc. Am.*, vol. 25, no. 2, pp. 327–334, 1953, doi: 10.1121/1.1907041.

[6] A. Cummings, "Sound transmission at sudden area expansions in circular ducts, with superimposed mean flow", *J. Sound Vib.*, vol. 38, no. 1, pp. 149-155, 1975, doi: 10.1016/s0022-460x(75)80024-1.

[7] M. L. Munjal, "Velocity ratio-cum-transfer matrix method for the evaluation of a muffler with mean flow", *J. Sound Vib.*, vol. 39, no. 1, pp. 105–119, 1975, doi: 10.1016/s0022-460x(75)80211-2.

[8] A. M. Cargill, "Low frequency acoustic radiation from a jet pipe—a second order theory", *J. Sound Vib.*, vol. 83, no. 3, pp. 339–354, 1982, doi: 10.1016/s0022-460x(82)80097-7.

[9] J. Ih and B. Lee, "Analysis of higher-order mode effects in the circular expansion chamber with mean flow", *J. Acoust. Soc. Am.*, vol. 77, no. 4, pp. 1377–1388, 1985, doi: 10.1121/1.392029.

[10] K. S. Peat, "The acoustical impedance at discontinuities of ducts in the presence of a mean flow", *J. Sound Vib.*, vol. 127, no. 1, pp. 123–132, 1988, doi: 10.1016/0022-460x(88)90353-7.

[11] J. B. Lawrie and I. D. Abrahams, "Acoustic radiation from two opposed semi-infinite coaxial cylindrical waveguides. II: separated ducts", *Wave motion*, vol. 19, no. 1, pp. 83–109, 1994, doi: 10.1016/0165-2125(94)90014-0.

[12] S. Föller and W. Polifke, "Identification of aero-acoustic scattering matrices from large eddy simulation. Application to a sudden area expansion of a duct", *J. Sound Vib.*, vol. 331, no. 13, pp. 3096–3113, 2012, doi: 10.1016/j.jsv.2012.01.004.

[13] J. B. Lawrie, "An infinite, elastic, cylindrical shell with a finite number of ring constraints", *J. Sound Vib.*, vol. 130, no. 2, pp. 189–206, 1989, doi: 10.1016/0022-460x(89)90549-x.

[14] M. C. Junger and D. Feit, "Sound, structures, and their interaction", *MIT press Cambridge*, MA, vol. 225, 1986, doi: 10.1016/0022-460x(87)90421-4.

[15] P. Stepanishen and R. A. Tougas Jr, "Transient acoustic pressure radiated from a finite duct", *J. Acoust. Soc. Am.*, vol. 93, no. 6, pp. 3074–3084, 1993, doi: 10.1121/1.405739.

[16] B. Zhang and I. D. Abrahams, "The radiation of sound from a finite ring-forced cylindrical elastic shell I. Wiener–Hopf analysis", *Proc. R. Soc. London. Ser. A Math. Phys. Sci.*, vol. 450, no. 1938, pp. 89–108, 1995, doi: 10.1098/rspa.1995.0073.

[17] C. Dutrion and F. Simon, "Acoustic scattering reduction using layers of elastic materials", *J. Sound Vib.*, vol. 388, pp. 53–68, 2017, doi: 10.1016/j.jsv.2016.10.034.

[18] Y. Qiao, H. Wang, X. Liu, and X. Zhang, "Acoustic radiation force on an elastic cylinder in a Gaussian beam near an impedance boundary", *Wave Motion*, vol. 93, p. 102478, 2020, doi: 10.1016/j.wavemoti.2019.102478.

[19] Z. Gong, W. Li, Y. Chai, Y. Zhao, and F. G. Mitri, "T-matrix method for acoustical Bessel beam scattering from a rigid finite cylinder with spheroidal endcaps", *Ocean Eng.*, vol. 129, pp. 507–519, 2017, doi: 10.1016/j.oceaneng.2016.10.043.

[20] G. S. Sharma, A. Skvortsov, I. MacGillivray, and N. Kessissoglou, "Acoustic performance of periodic steel cylinders embedded in a viscoelastic medium", *J. Sound Vib.*, vol. 443, pp. 652–665, 2019, doi: 10.1016/j.jsv.2018.12.013.

[21] J. V. Venås and T. Kvamsdal, "Isogeometric boundary element method for acoustic scattering by a submarine", *Comput. Methods Appl. Mech. Eng.*, vol. 359, p. 112670, 2020, doi: 10.1016/j.cma.2019.112670.

[22] K. Premkumar and B. V Manikandan, "Bat algorithm optimized fuzzy PD based speed controller for brushless direct current motor", *Eng. Sci. Technol. an Int. J.*, vol. 19, no. 2, pp. 818–840, 2016, doi: 10.1016/j.jestch.2015.11.004.

[23] K. Premkumar and B. V Manikandan, "Speed control of Brushless DC motor using bat algorithm optimized Adaptive Neuro-Fuzzy Inference System", *Appl. Soft Comput.*, vol. 32, pp. 403–419, 2015, doi: 10.1016/j.asoc.2015.04.014.